ACES Asian Chemical Editorial Society

DOI: 10.1002/asia.201501253

CHEMISTRY
AN ASIAN JOURNAL
Full Paper

DNA Repair

O^6-Alkylguanine DNA Alkyltransferase Repair Activity Towards Intrastrand Cross-Linked DNA is Influenced by the Internucleotide Linkage

Derek K. O'Flaherty and Christopher J. Wilds*[a]

Abstract: Oligonucleotides containing an alkylene intrastrand cross-link (IaCL) between the O^6-atoms of two consecutive 2′-deoxyguanosines (dG) were prepared by solid-phase synthesis. UV thermal denaturation studies of duplexes containing butylene and heptylene IaCL revealed a 20 °C reduction in stability compared to the unmodified duplexes. Circular dichroism profiles of these IaCL DNA duplexes exhibited signatures consistent with B-form DNA. Human O^6-alkylguanine DNA alkyltransferase (hAGT) was capable of repairing both IaCL containing duplexes with slightly greater efficiency towards the heptylene analog. Interestingly, repair efficiencies of hAGT towards these IaCL were lower compared to O^6-alkylene linked IaCL lacking the 5′-3′-phosphodiester linkage between the connected 2′-deoxyguanosine residues. These results demonstrate that the proficiency of hAGT activity towards IaCL at the O^6-atom of dG is influenced by the backbone phosphodiester linkage between the cross-linked residues.

Introduction

DNA insults may be incurred by environmental agents, endogenous metabolic processes and chemotherapeutic drugs.[1,2] Some chemotherapy regimens exploit the use of bifunctional electrophilic agents, which act on DNA to produce lesions and interfere with vital processes such as DNA replication.[3] Stalling these processes or modification of the information encoded in DNA can have severe effects on the cell. Bifunctional electrophilic agents can form adducts in DNA which link the atoms of two nucleotides on the same (intra) or opposing (inter) strands. Interstrand cross-links (ICL) in DNA are particularly cytotoxic given that the unwinding of the individual strands is prevented, which impedes cellular proliferation.[3–5] Although damage occurs on one strand for intrastrand cross-linked (IaCL) DNA, information content and structure can be affected. Cisplatin, a platinum-based drug used for the treatment of some forms of cancer, predominantly introduces lesions that are IaCL in nature.[6–10] Busulfan[11] and mitomycin C[12,13] are examples of bis-electrophilic agents which can introduce IaCL lesions in DNA, and can lead to the blockage of DNA replication and activation of apoptosis.[14,15]

O^6-Alkyl-2′-deoxyguanosine adducts can be formed by exposure to carcinogenic agents such as nitrosamines and chemotherapeutic alkylating agents such as temozolomide.[16] This class of lesions can induce transitional mutations via proficient base pairing with thymidine during DNA replication,[17] and the activation of mismatch repair can result in futile excision-resynthesis, ultimately leading to apoptosis.[18,19] Our group has shown that human O^6-alkylguanine DNA alkyltransferase (hAGT) is capable of repairing certain ICL.[20–24] The primary role of AGTs is to remove alkyl lesions found at the O^6-position of dG and, to a lesser extent, at the O^4-position of dT.[25] In the active site of the protein, the alkyl lesion becomes transferred to an activated cysteine, rendering the AGT protein irreversibly inactivated and ultimately degraded in vivo by the ubiquitin pathway.[26,27]

The human AGT (hAGT) variant is capable of repairing butylene and heptylene ICL linking the O^6-positions of dG residues in a directly opposed fashion, as well as in a 5′-GNC motif.[20,21] Recently, we demonstrated that hAGT could also act on a DNA duplex containing an IaCL on one of the strands consisting of an alkylene functionality attaching the O^6-atoms of two dG residues that lack a phosphodiester linkage in the backbone between them (Figure 1 A).[28] hAGT was proficient towards removing the lesion, with almost complete consumption observed for a heptylene-linked substrate within 60 min. These results prompted us to explore AGT activity towards the IaCL containing a phosphodiester linkage at this site (Figure 1 B).

In the current investigation, a methodology to introduce this O^6-2′-deoxyguanosine-alkylene-O^6-2′-deoxyguanosine IaCL (O^6-dG-alkylene-O^6-dG, Figure 1 B) was developed. The influence of this IaCL modification in a DNA duplex was assessed by UV thermal denaturation and circular dichroism. Repair of this IaCL DNA by a variety of AGTs (human and *E. coli*) was evaluated. Given the efficient action of hAGT on the IaCL DNA probes lacking the phosphodiester linkage between the 3′-

[a] D. K. O'Flaherty, Prof. C. J. Wilds
Department of Chemistry&Biochemistry
Concordia University
7141 Sherbrooke St. West, Montréal, Québec (Canada)
E-mail: Chris.Wilds@concordia.ca

Supporting information for this article is available on the WWW under http://dx.doi.org/10.1002/asia.201501253.

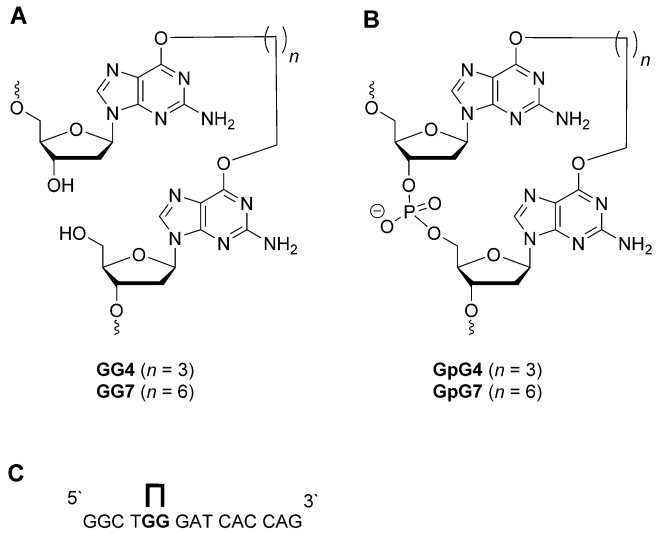

Figure 1. Structures of O^6-2′-deoxyguanosine-alkylene-O^6-2′-deoxyguanosine intrastrand cross-link (**A**) lacking or (**B**) containing the phosphodiester linkage and (**C**) the oligonucleotide sequence indicating the position of the laCLs (shown by **GG**).

and 5′-*O* groups of the O^6-alkylene linked dG residues, these new laCL probes may aid in the understanding of backbone flexibility versus rigidity imposed by the phosphodiester linkage on repair of laCL DNA. Butylene and heptylene laCL linkages were chosen on the basis that busulfan can react with DNA to produce butylene-linked laCL at the N7-positions of 5′-d(GA) and 5′-d(GG) sequences.[11] To be noted is that this specific laCL between the O^6-positions of 5′-d(GG) sequences have not been identified to occur upon exposure of DNA to bifunctional alkylating agents. The heptylene linkage was also prepared as the sulfamate hepsulfam has been demonstrated to introduce an ICL at the N7-positions of 2′-deoxyguanosine in a 5′-d(GNC) motif.[29] The processing of this laCL by hAGT will contribute to our understanding of the substrate range that can undergo repair by this protein.

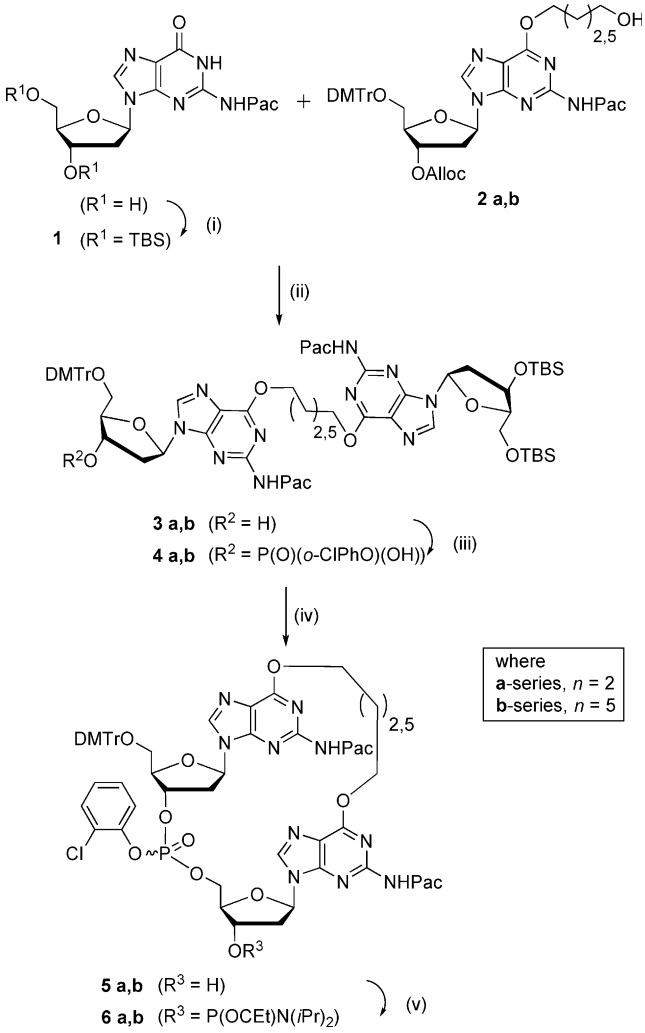

Scheme 1. Reagents and conditions: (i) TBS-Cl (2.5 eq), Im (5.0 eq), DMAP (cat), DCM, 21 °C, 16 h. (ii) 1. **1** (1.0 eq), **2a** or **2b** (1.1 eq), Ph_3P (1.2 eq), DIAD (1.2 eq), dioxane, 21 °C, 16 h. 2. $[Pd(Ph_3P)_4]$ (0.2 eq), Ph_3P (0.4 eq), $nBuNH_2$ (7 eq), HCOOH (7 eq), THF, 21 °C, 30 min. (iii) 2-chlorophenyl dichlorophosphate (5 eq), 1,2,4-triazole (10 eq), NEt_3 (10 eq), THF, Py, 21 °C, 2 h. (iv) 1. TBAF (10 eq), THF, 21 °C, 6 h. 2. MSNT (5 eq), Py, 21 °C, 16 h. (v) Cl-P(OCEt)N(*i*Pr)$_2$ (1.2 eq), DIPEA (1.5 eq), THF, 21 °C, 30 min.

Results and Discussion

Synthesis and characterization of laCL DNA

The structure of the O^6-dG-alkylene-O^6-dG cross-links containing a phosphodiester linkage between the 5′- and 3′-*O* atoms (**GpG4** and **GpG7**) and their position in the oligonucleotide sequence investigated in this study is shown in Figure 1. The synthesis approach for cross-linked amidites **6a** and **6b** is shown in Scheme 1 and began with commercially available N^2-phenoxyacetyl-2′-deoxyguanosine. This material was azeotropically dried with anhydrous pyridine, followed by bis-silylation at the 3′ and 5′ hydroxyl functionalities. Compounds **2a** and **2b** were prepared according to procedures described previously by our group.[21] Dimers **3a** and **3b** were produced using the Mitsunobu reaction of mono-adducts **2a** and **2b**, respectively, with compound **1** followed by the Pd^0-catalyzed removal of the allyloxycarbonyl group. Fully-protected versions of **3a** and **3b** were particularly difficult to isolate in high purity due to co-elution with mixtures of triphenylphosphine/triphenylphosphine oxide. The subsequent removal of the allyloxycarbonyl group, deprotecting the 3′-hydroxyl functionality, facilitated the chromatographic purification of the desired dimers (**3a** and **3b**). Phosphorylation of **3a** and **3b** was accomplished by adapting reported approaches which produced dimers **4a** and **4b**, respectively.[30–32] Solubility proved to be an issue during the washing (work-up) stages of the latter intermediates, particularly for **4a**. The introduction of NEt_3 in the work-up solvent alleviated this issue as the corresponding triethylammonium phosphate salts are generally more soluble in organic solvents. The ring-closing reaction to access **5a** and **5b** was accomplished according to a procedure described previously.[30] The use of MSNT (MSNT = 1-(2-mesitylenesulfonyl)-3-nitro-1*H*-1,2,4-triazole) as the condensing reagent favors attack by the 5′-OH, as opposed to the 3′-OH, of the desilylated resi-

due.[30–32] We hypothesized that these transformations would occur more quickly for our system, which we tested on starting material **4a**. First, the desilylation reaction was reduced to 1 h (as opposed to 6 h), and the cyclization reaction time was reduced to 4 h compared to 16 h with no significant yield differences observed (51% and 52% for shorter and longer reaction times, respectively). For the heptylene analogue **4b**, a cyclization reaction time of 16 h was used. Phosphoramidites **6a** and **6b** were synthesized according to previously described procedures.[28] In our hands, phosphoramidite products of greater purity are generally attained using chromatography, relative to precipitation using hexanes. However, we initially resorted to precipitation using hexanes for isolating phosphoramidites **6a** and **6b** given the low mobility observed for these dimers by TLC. ^{31}P NMR spectroscopic analysis revealed sharp signals in the region of 148–150 ppm characteristic of phosphoramidites. Compounds **6a** and **6b** were further characterized by high-resolution mass spectrometry (HRMS), and the masses observed were in agreement with the expected values.

The IaCL DNA synthesis employed either cyclized dimer phosphoramidite **6a** or **6b**, which differed only in their respective alkylene linker length. The presence of a single DMTr group and single phosphoramidite moiety on the dimer scaffolds rendered a straightforward construction of the IaCL DNA. Assembly of oligonucleotides **GpG4** and **GpG7** by automated solid-phase synthesis was carried out according to previous published procedures used to prepare ICL and IaCL DNA containing similar modifications.[21,28] Coupling wait times for phosphoramidites **6a** and **6b** were extended to 10 min, relative to 2 min for standard 3′-*O*-phosphoramidites, in order to ensure efficient coupling of the dimers to the nascent oligomer. **GpG4** and **GpG7** were deprotected and cleaved from the solid support using a protocol described by Glen Research (aqueous NH_4OH (28%) for 17 h at room temperature with gentle rocking and an additional 4 h at 55 °C) with no detectable degradation of the cross-link observed by SAX-HPLC (see the Supporting Information). Failure sequences due to incomplete couplings of **6a** or **6b** were well-resolved from desired products by SAX-HPLC. This was also observed for shorter sequences that were prepared (12-mer, data not shown). MS analysis of the **GpG4** and **GpG7** revealed deconvoluted masses in agreement with the expected masses (values shown in Table 1 and spectra shown in the Supporting Information). Further characterization by enzymatic digestion followed by RP-HPLC showed the appearance of a new peak with retentions of 9.2 min and 14.7 min for the butylene and heptylene 2′-deoxyguanosine adducts, respectively (see the Supporting Information). The retention of these dimers was significantly lower compared with those observed for the enzymatic digestion of **GG4** and **GG7** (16.4 min and 24.8 min),[28] respectively, suggesting incomplete digestion near the cross-linked site, as previously observed for other DNA modifications.[33,34]

Table 1. Retention time and mass spectrometry data for **GpG4** and **GpG7**.

Oligomer	Retention time [min]	Mass	
		Expected	Observed
GpG4	21.1	4672.1	4673.0
GpG7	21.6	4714.2	4715.1

UV thermal denaturation and circular dichroism studies of IaCL DNA

The influence of the **GpG4** and **GpG7** IaCL on duplex stability with the complementary DNA sequence, relative to the native duplex and the more "flexible" IaCL **GG4** and **GG7** (reported previously), was assessed by UV thermal denaturation experiments. The thermal denaturation profiles of the IaCL containing DNA duplexes were monophasic with T_m values of 45, 48 and 68 °C for **GpG4**, **GpG7** and the unmodified duplex, respectively (Figure 2). Presence of a single O^6-methyl-dG insert in a DNA duplex resulted in a T_m reduction of approximately 18 °C and two inserts dropped the value by 40 °C, compared to unmodified sequences.[35,36] The influence of two O^6-alkylated dG residues for the butylene- and heptylene-linked IaCL (**GpG4** and **GpG7**) resulted in an overall reduction in T_m by 20–23 °C relative to the control, which was lower than expected. The reduction in stability is most likely attributed to the disruption of hydrogen bonding between the alkylated 2′-deoxyguanosines, containing the flexible alkylene linkers, with their paired 2′-deoxycytidines that may result in local and global structural perturbations. Interestingly, these values were comparable to the IaCL analogs which lack the phosphodiester linkage (46 °C and 48 °C for **GG4** and **GG7**, respectively). We had originally hypothesized that the added flexibility and lack of the anionic phosphodiester linkage at the cross-linked site for the **GG4**- and **GG7**-containing duplexes may have reduced repulsion effects relative to **GpG4** and **GpG7**, resulting in higher T_m values, which was not the case. This would suggest that the electrostatic repulsion involved in duplexes containing **GpG4** and **GpG7** is compensated for by other contributing factors. Towards this end, we performed van't Hoff experiments to determine the thermodynamic parameters in order to evaluate if the decrease in T_m with respect to the unmodified control could be attributed to an enthalpic or entropic cost (see the

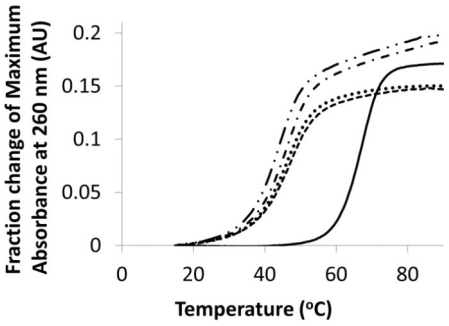

Figure 2. Fraction change of maximum absorbance at 260 nm (A_{260}) versus temperature [°C] profiles of duplexes containing **GG4** (···),[28] **GG7** (-----),[28] **GpG4** (–··), **GpG7** (–·–·) and unmodified DNA (——).

Supporting Information for T_m profiles and values). The data suggest that the reduction in stability due to the presence of the flexible IaCL and phosphodiester linkage was generally attributed to an enthalpic cost. There seemed to be an entropic cost for **GG7**- and **GpG4**-containing duplexes, whereas **GG4**- and **GpG7**-containing duplexes revealed an entropic gain relative to the unmodified control.

Circular dichroism (CD) spectroscopy was performed to determine the global structural influence of the **GpG4** and **GpG7** IaCL in the DNA duplex. CD profiles of these modified duplexes displayed signatures consistent with B-form DNA with maxima near 280 nm, cross-overs near 250–260 nm, and minima around 240 nm (shown in Figure 3). However, the profile for

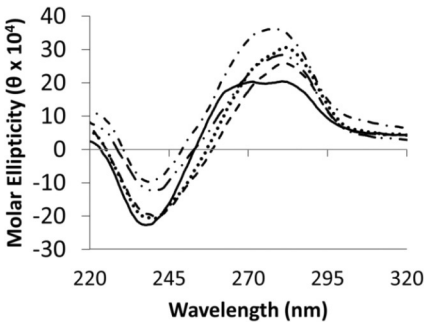

Figure 3. Circular dichroism spectra of IaCL duplexes, **GG4** (-----),[28] **GG7** (···),[28] **GpG4** (–•–•), **GpG7** (–••) and unmodified DNA (——).

duplexes containing the **GpG4** IaCL displayed a slight blue shift of the spectra relative to the unmodified control. Nonetheless, these results indicate that minor global structural distortions were induced by the presence of the alkylene IaCL in the DNA duplexes. Similar findings were observed for the "flexible" IaCL DNA (**GG4** and **GG7**) and duplexes containing monoadducts at the O^6-atom of dG (data shown only for **GG4** and **GG7** in Figure 3). Duplexes containing the **GpG4** and **GpG7** IaCL (and unmodified control) were geometry-optimized using the AMBER force field (see the Supporting Information for the models). In both cases, the alkylene linker protruded into the major groove, with a slight widening observed in addition to buckling of the 5′-end O^6-alkylated dG nucleobase. The buckling effect was more pronounced for **GpG4** compared to **GpG7**, relative to the "flexible" **GG4**, **GG7** and control. The molecular models suggest that the presence of the cross-link does not greatly distort the global structure of the duplex, consistent with the small variation in the CD profiles observed for **GpG4** and **GpG7**. High-resolution structures of duplexes containing **GpG4** or **GpG7** are currently being investigated by a combination of molecular dynamics and high-field NMR experiments.

AGT-mediated repair of IaCL DNA

Four AGT proteins (hAGT, OGT, an S134P OGT variant, and Ada-C) were interrogated against the single strands **GG4** and **GG7**, as well as duplexes containing **GpG4** and **GpG7**. The repair of duplexes containing **GG4** and **GG7** has been described previously.[28] The modified strand was radiolabeled using γ-[^{32}P]ATP and either used as is or annealed with a 10% molar excess of the complementary sequence followed by incubation for 16 h at 37 °C with the AGT protein of interest (2 pmol DNA and either 10 pmol or 60 pmol protein). Repair reactions were quenched and boiled to prevent complexation before loading onto the denaturing gel. Analysis of the AGT activity upon single-stranded **GG4** and **GG7** revealed that only the human variant was capable of removing the lesion at 5-fold protein equivalence (see the Supporting Information). Interestingly, repair efficiencies of the **GG4** and **GG7** single strands by hAGT were in agreement with repair of duplexes containing the IaCL DNA, respectively.[28] No repair was observed, however, for other AGTs tested at 5-fold protein equivalence, whereas minimal repair (<15%) was observed by OGT, Ada-C and OGT S134P at 30-fold protein equivalence (see the Supporting Information). Repair studies conducted on double-stranded **GpG4** and **GpG7** revealed that only hAGT reacted with these IaCL, with slightly higher efficiency towards the **GpG7** (lanes 4 and 10 in Figure 4). Surprisingly, the levels of repair were much lower for the IaCL DNA containing the phosphodiester linkage compared to both the single strands and duplexes containing the flexible **GG4** and **GG7** IaCL.[28] The **GG4** and **GG7** duplex substrates were virtually entirely consumed (4 and 5% IaCL substrate remaining, respectively) compared to 74% and 64% substrate remaining for **GpG4** and **GpG7** duplexes, respectively, at 30-fold excess protein. OGT and Ada-C were incapable of repairing the IaCL DNA studied (10 pmol protein and 2 pmol DNA), which was not surprising given their inefficient repair of

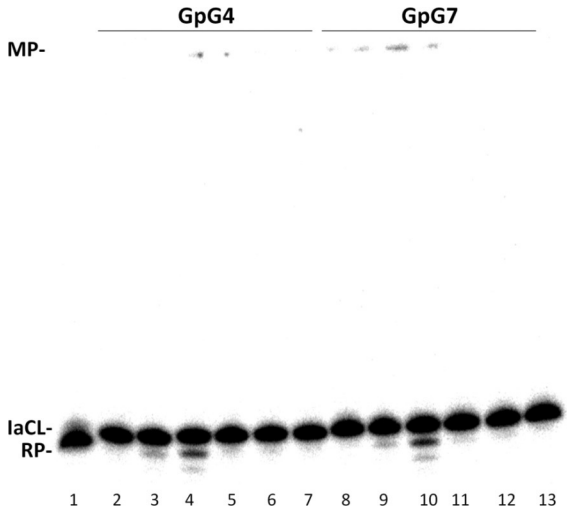

Figure 4. Repair of **GpG4** and **GpG7** by hAGT, OGT, Ada-C, and OGT S134P. Denaturing PAGE of repair reactions as described in the Experimental Section. Lane 1, 2 pmol control unmodified DNA + 10 pmol hAGT; lane 2, 2 pmol **GpG4**; lane 3, 2 pmol **GpG4** + 10 pmol hAGT; lane 4, 2 pmol **GpG4** + 60 pmol hAGT; lane 5, 2 pmol **GpG4** + 10 pmol OGT; lane 6, 2 pmol **GpG4** + 10 pmol Ada-C; lane 7, 2 pmol **GpG4** + 10 pmol OGT S134P; lane 8, 2 pmol **GpG7**; lane 9, 2 pmol **GpG7** + 10 pmol hAGT; lane 10, 2 pmol **GpG7** + 60 pmol hAGT; lane 11, 2 pmol **GpG7** + 10 pmol OGT; lane 12, 2 pmol **GpG7** + 10 pmol Ada-C; lane 13, 2 pmol **GpG7** + 10 pmol OGT S134P. To be noted is a faint band below the repair product in lanes 4 and 10, which may be an artefact from the lengthy electrophoresis.

lesions larger than a methyl group at the O^6-atom of dG. Although OGT is capable of repairing larger O^4-alkylated thymidine mono-adducts (but not ICL DNA),[22] OGT demonstrated no repair activity towards **GpG4** and **GpG7**, even at higher AGT ratios (Supporting Information). The OGT S134P variant[24] demonstrated no activity towards these IaCL DNA duplexes as well.

Complete repair of these IaCL DNA (**GpG4** and **GpG7**) by hAGT would begin with a reaction to generate a median product (**MP** in Figure 4) consisting of a hAGT-DNA cross-linked species. Repair of this hAGT-DNA **MP** by a second AGT protein would generate the completely repaired product (**RP** in Figure 4). Repair assays of various AGTs with **GpG4** and **GpG7** were performed and the products analyzed by denaturing gel electrophoresis (Figure 4). Lanes 2 and 8 contain the **GpG4** and **GpG7** ssDNA, respectively. Lane 1 contains the unmodified control DNA strand of identical sequence as **GpG4** and **GpG7**. The control DNA strand migrated slightly faster compared to the IaCL DNA, which indicated that resolution of the IaCL DNA and repaired DNA by electrophoresis was feasible. Lanes 3 and 9 display the product of the repair reaction for **GpG4** and **GpG7** (2 pmol) with hAGT (10 pmol), respectively. Lanes 4 and 10 display similar reactions with higher hAGT concentrations (60 pmol) for **GpG4** and **GpG7**, respectively. Two new bands are observed for the reaction of **GpG4** and **GpG7** with hAGT; one which migrates much slower and another that migrates slightly faster. The slowly migrating band can be attributed to the formation of hAGT covalently bound to the damaged DNA (**MP**), as observed previously with AGT repair of O^6-dG-alkylene-O^6-dG IaCL and ICL DNA.[20, 22, 23, 28] The faster migrating band corresponded to the **RP**. The proposed repair pathway is illustrated in Figure 5.

The amount of repair observed for the **GpG4** IaCL was similar to that of duplexes containing an O^6-dG-butylene-O^6-dG ICL

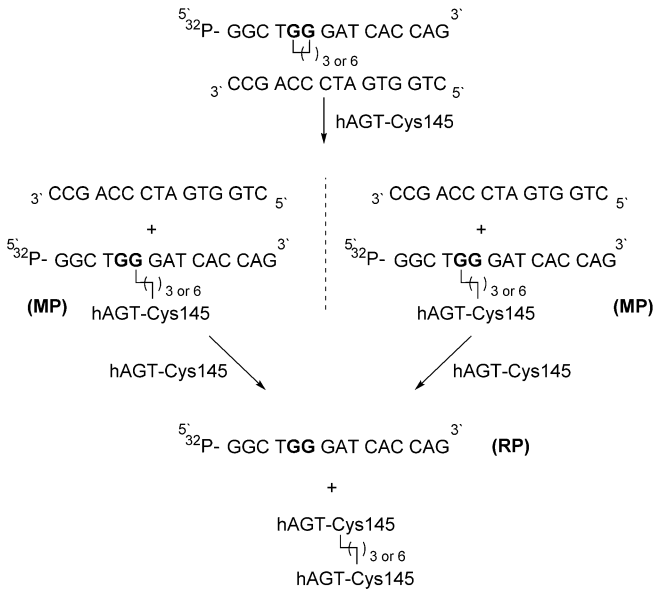

Figure 5. Proposed repair pathway of IaCL species by wild-type hAGT (**MP**, median product; **RP**, repair product).

(**XL4**, with approximately 65–70% of ICL DNA left unrepaired), whereas repair of the duplex containing a heptylene ICL (**XL7**) surpassed that of the **GpG7** (approximately 43% and 65% remaining of unrepaired **XL7** and **GpG7**, respectively) (see Supporting Figure 33 for chemical structures of **XL4** and **XL7**). Previously, Abdu and co-workers described poor hAGT-mediated repair of DNA containing a conformationally locked *anti* analogue of O^6-methyl-2′-deoxyguanosine.[37] Our group has also observed that various AGTs were incapable of repairing DNA containing conformationally locked analogues of O^4-alkyl-thymidine (data not shown) where a methylene group at the O^4-position is *anti* relative to the N3-atom. Together, the latter two examples suggest that repair by AGTs may be dependent on lesion conformation, whereby attack by the active site Cys thiolate anion only proceeds if the α-carbon of the lesion is positioned correctly. The orientation of the alpha carbons of the O^6-alkylene linkers in **GpG4** and **GpG7** may not have the conformational freedom to adopt an optimal orientation for successful repair, which may explain the large discrepancies observed in the repair of the IaCL DNA containing the phosphodiester linkage. The alkylene linkers in these IaCL, lacking the phosphodiester linkage, may be more flexible and are thus capable of adopting multiple different conformations relative to the IaCL DNA investigated in this study. Fang and coworkers generated a molecular model of hAGT in complex with an O^6-dG-heptylene-O^6-dG ICL DNA, which suggested that the preferential repair of longer ICL DNA by hAGT is due to the shape of the hAGT active site once the DNA is bound (similar to a "tunnel").[20] The longer heptylene linker in **GpG7** may be accommodated more readily into the "tunnel" of the active site, allowing for positioning of the α-carbon near the C145 residue, compared to the more strained butylene linker in **GpG4**. This may account for the reason why the heptylene adducts are repaired more efficiently by hAGT. However, the length of the linker affected hAGT repair more drastically in the case of ICL DNA (**XL7** versus **XL4**) and IaCL lacking the phosphodiester linkage (**GG7** versus **GG4**), with much greater repair efficiency observed for the heptylene analogues. Much of our understanding of the AGT repair mechanism is derived from crystal structures of hAGT C145S bound to damage-containing DNA (hAGT with DNA containing an O^6-MedG insert and another of hAGT covalently cross-linked with DNA containing a N^1,O^6-ethanoxanthosine insert).[40] Both structures reveal conformational changes occurring in the DNA during the repair process with minimal changes in the protein structure. Similar findings were observed for *E. coli* Ada.[38] The alkylated nucleotide is flipped into the protein active site allowing for attack of the activated thiolate anion of Cys145. In the case of **GpG7** and **GpG4**, the alkylene linkers could be thought of as part of a larger ring system, which may prevent the necessary entry of the alpha carbon into the active site in order for alkyl group transfer. This may be a result from rotation of the O^6-alkylated linked dG residue, which is covalently attached to the O^6-atom of the adjacent dG residue.

Time course assays were performed using 60 pmol hAGT and 2 pmol of either **GpG4** or **GpG7** duplex substrates by quantifying the amounts of unrepaired, **MP** and **RP** products

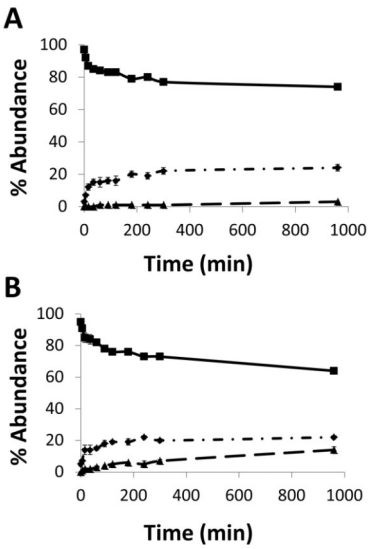

Figure 6. Time course repair assay of **GpG4** (top) and **GpG7** (bottom) by hAGT displaying a faster repair of **GpG7**. Graphical illustrations display abundances [%] of **MP** (-----), **RP** (–•–•)and substrate (——) over time (min).

(see the Supporting Information for the denaturing PAGE). The data, summarized in Figure 6, reveals that **GpG4** was depleted by hAGT at a slower rate with approximately 20% repair occurring in 4 h whereas similar levels of repair for **GpG7** required 1 h. The formation of the **RP** reached a plateau after similar reaction times for **GpG4** and **GpG7** with values within 20–25%. The formation of the **MP**, on the other hand, plateaued at a higher value for duplexes containing **GpG7** (14%) compared to **GpG4** (3%). The faster repair of **GpG7** compared to **GpG4** is probably due to the added flexibility imparted from the longer alkylene linker, which may allow for more optimal rotation of the damaged nucleotide into the protein active site. The geometrically optimized molecular models of **GpG4**, **GpG7** and unmodified duplexes revealed an O^6-O^6 distance of 3.0, 3.2, and 3.5 Å, respectively. An increase in base tilting observed for **GpG4** relative to **GpG7** suggests that the butylene adduct is more strained relative to the heptylene adduct, which could account for the greater repair observed for **GpG7** relative to **GpG4**. Comparison of the **GpG4** and **GpG7** structures to **GG4** and **GG7** revealed an increase in buckling for laCL DNA duplexes containing the phosphodiester linkage. Greater repair was also observed for **XL7** versus **XL4** ICL DNA by hAGT.[21] Repair of **GpG4** duplexes by hAGT proceeded slightly faster compared to **XL4**, whereas repair of **XL7** occurred more quickly compared to **GpG7** duplexes, showing a clear distinction in the efficiency of hAGT towards processing these forms of DNA modifications despite the alkylene linker of the laCL residing on one strand only.

The time course assay revealed reduced reaction rates for processing of **GpG4** and **GpG7** laCL duplexes compared to those containing **GG4** and **GG7** by hAGT. After a repair reaction time of 4 h, 80% and 73% of **GpG4** and **GpG7** remained, respectively, whereas virtually all of **GG4** and **GG7** substrates were depleted by hAGT (at 30-fold excess of protein). As stated previously, this drastic difference imparted by the presence of the phosphodiester linkage may likely be the result of the alkylene linkers found in **GpG4** and **GpG7** adopting less reactive conformations, which has been proposed for other O^6-alkylated-dG lesions.[39]

In our previous report of the repair of duplexes containing the **GG4** and **GG7** laCL by hAGT, we proposed that the phosphorylation of the damaged strand occurred at the 5′-terminus of the oligomer. A more detailed analysis of the repair event revealed that T4 PNK is capable of phosphorylating the internal 5′-hydroxyl group as well (see the Supporting Figures 25–27). To validate that T4 PNK could in fact phosphorylate both positions, T4 PNK and a three-fold excess of ATP were incubated with either **GG4** or **GG7**. Mass spectral analysis revealed the presence of mono- and bis-phosphorylated products (see Supporting Figures 21–22). To help decipher the repair pathway of **GG4** and **GG7**, a mixture of γ-[^{32}P]ATP (1 μL, 10 μCi) and non-radioactive ATP (3-fold excess) was used to radiolabel the damaged strand DNA. The total repair assay of **GG4** and **GG7** resulted in different ratios of **RP** and **MP**, with substrate consumption levels in agreement with those previously observed (see Supporting Figure 27 for the denaturing gel and Supporting Figure 34 for the potential repair pathway). The variance observed in the **RP** and **MP** levels may have resulted from the mixture of mono- and bis-phosphorylated products of **GG4** and **GG7**.

The radioactivity-based assay has the limitation of only monitoring the DNA species, which prompted us to perform an SDS-PAGE analysis of the reaction to analyze the various proteinaceous products formed (Figure 7).[23] Lane 1 contains the

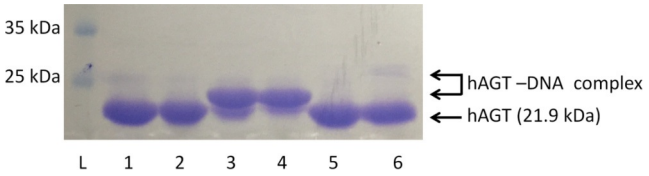

Figure 7. 12% SDS-PAGE of hAGT mediated repair of **GG4**, **GG7**, **GpG4**, and **GpG7**. Repair of 600 pmol laCL DNA by 600 pmol hAGT for 16 h at 37 °C: lane L, unstained protein molecular weight marker; lane 1, hAGT; lane 2 unmodified control DNA + hAGT reaction; lane 3 GG4 + hAGT reaction; lane 4 GG7 + hAGT reaction; lane 5 GpG4 + hAGT reaction; lane 6 GpG7 + hAGT reaction.

hAGT protein alone, whereas lanes 2–6 contain hAGT with unmodified DNA, **GG4**, **GG7**, **GpG4**, and **GpG7**, respectively (600 pmol protein incubated with 600 pmol DNA for 16 h at 37 °C). Lanes 3 and 4 both show the presence of two bands, of which one is minor with a faster migration similar to the unreacted hAGT protein. The major, slower migrating band is presumably the AGT-DNA covalent complex, and is in agreement with our radioactivity-based repair assay and previous preparations of AGT-DNA complexes using ICL DNA.[23] Interestingly, the reaction between a 1:1 molar equivalence of **GG4** or **GG7** with hAGT yielded almost quantitative conversion to the DNA-protein covalent complex. Lane 5 displays the lack of **GpG4** repair by hAGT whereas lane 6 reveals the appearance of a faint band with lower mobility compared to the hAGT pro-

tein (major band), consistent with the formation of a covalently linked AGT-DNA species.

The in vitro assay results demonstrate that IaCL DNA containing butylene and heptylene linkers are repaired by hAGT adding to our knowledge of the substrate range that this protein can act upon. IaCLs can be introduced in DNA by different bifunctional alkylating agents such as busulfan, however, the O^6-position of dG is not the major site of adduct formation. McManus and coworkers previously showed that AGT-deficient CHO cells are sensitive to killing by hepsulfam. It was also shown that hAGT can protect CHO cells, in part, against hepsulfam exposure, but not busulfan. Our preliminary results are consistent with this finding as more efficient hAGT repair is observed for the heptylene versus butylene IaCL adducts.

X-ray crystallography studies of hAGT bound to damaged DNA have shown that Tyr114 is necessary for flipping of the damaged nucleotide into the active site of the protein.[40] Y114F and Y114A hAGT mutants have reduced activity towards O^6-alkylated-dG lesions highlighting the important role of Tyr114. In the current study, the presence of the phosphodiester linkage between the O^6-linked IaCL (**GpG4** and **GpG7**) reduced the repair efficiency by hAGT compared to those lacking the phosphodiester group (**GG4** and **GG7**). The basis for the interaction of Tyr114 with the 3′-phosphate group of the target nucleotide has been proposed as being steric[40] or electronic[41] in nature. The interaction of the phosphate group of **GpG4** and **GpG7** with Tyr114 may be unfavorable, which contributes to lower repair efficiencies observed by hAGT. Investigation of the AGT repair of O^6-dG-alkylene-O^6-dG IaCL containing other backbone bio-isosteric linkages, such as formacetal group,[42] may contribute to probing the contributions of the sterics and electronics of Tyr114 towards AGT-mediated repair.

One highlight feature of this study is the efficient repair of single-stranded **GG7** by hAGT with only 5-fold excess protein (and similar efficiencies for **GG4** at 60-fold excess hAGT). Given the lack of the phosphodiester linkage at the cross-link site, repair of the IaCL cleaves the DNA into two smaller DNA fragments. This system may be used as a functional irreversible switch for novel molecular nanotechnology devices. Recently, there have been a number of reports describing the activity of AGT towards various DNA structures and applications in protein tagging.[43–45] The integration of these IaCL modifications into a device would potentially benefit from orthogonality, and little crosstalk with other switch mechanisms such as pH, UV irradiation, and toehold-mediated strand-displacement mechanisms. Other types of flexible IaCL such as those linking the O^6-atom of dG to the O^4-atom of dT in DNA sequences are currently being investigated for such applications.

Conclusions

Cyclic nucleoside dimers containing an alkylene linkage between the O^6-atoms of two 2′-deoxyguanosines were synthesized and the corresponding phosphoramidites were incorporated into DNA by solid-phase synthesis to produce IaCL DNA. Thermal denaturation analysis of duplexes containing these butylene and heptylene IaCL were found to result in a reduction in the T_m by about 20 °C relative to the control. Circular dichroism and molecular modeling suggested minimal global perturbation in the duplex structure. Both **GpG4** and **GpG7** were repaired moderately by hAGT, with slightly greater efficiency for the heptylene versus the butylene linker. IaCL DNA lacking the phosphodiester group at the cross-link site (**GG4** and **GG7**) were repaired with much greater efficiency. These results contribute an ongoing investigation of AGT to act upon modified DNA structures.

Experimental Section

All experimental methods and additional data including ^{1}H, ^{13}C and ^{31}P NMR spectra of compounds, HPLC chromatographs and MS spectra of oligonucleotides, T_m curves, molecular models and repair data can be found in the Supporting Information document.

Acknowledgements

The authors are grateful to Dr. Anthony E. Pegg (Pennsylvania State University) for the plasmid encoding the wild-type hAGT, OGT and Ada-C genes. We are also grateful to Dr. Francis McManus and Lauralicia Sacre for helpful discussions concerning the repair assays and Dr. Anne Noronha for assistance with solid phase synthesis. This work was supported by grants from the Natural Sciences and Engineering Research Council of Canada (NSERC, Grant No. 299384-2011) and the Canada Research Chair Program (Grant No. 950-213807). D.K.O. is the recipient of a Canada Graduate Scholarship (CGS) from NSERC.

Keywords: DNA damage · DNA repair · intrastrand cross-link · O^6-alkylguanine DNA alkyltransferase · oligonucleotides

[1] N. Shrivastav, D. Li, J. M. Essigmann, *Carcinogenesis* **2010**, *31*, 59–70.
[2] J. H. Houtgraaf, J. Versmissen, W. J. van der Giessen, *Cardiovasc. Revasc. Med.* **2006**, *7*, 165–172.
[3] D. M. Noll, T. M. Mason, P. S. Miller, *Chem. Rev.* **2006**, *106*, 277–301.
[4] M. L. Dronkert, R. Kanaar, *Mutat. Res.* **2001**, *486*, 217–247.
[5] D. Fu, J. A. Calvo, L. D. Samson, *Nat. Rev. Cancer* **2012**, *12*, 104–120.
[6] A. Eastman, *Biochemistry* **1986**, *25*, 3912–3915.
[7] A. Eastman, *Pharmacol. Ther.* **1987**, *34*, 155–166.
[8] K. Chvalova, V. Brabec, J. Kasparkova, *Nucleic Acids Res.* **2007**, *35*, 1812–1821.
[9] R. Olinski, A. Wedrychowski, W. N. Schmidt, R. C. Briggs, L. S. Hnilica, *Cancer Res.* **1987**, *47*, 201–205.
[10] L. A. Zwelling, T. Anderson, K. W. Kohn, *Cancer Res.* **1979**, *39*, 365–369.
[11] T. Iwamoto, Y. Hiraku, S. Oikawa, H. Mizutani, M. Kojima, S. Kawanishi, *Cancer Sci.* **2004**, *95*, 454–458.
[12] R. Bizanek, B. F. McGuinness, K. Nakanishi, M. Tomasz, *Biochemistry* **1992**, *31*, 3084–3091.
[13] S. M. Rink, R. Lipman, S. C. Alley, P. B. Hopkins, M. Tomasz, *Chem. Res. Toxicol.* **1996**, *9*, 382–389.
[14] V. Marini, P. Christofis, O. Novakova, J. Kasparkova, N. Farrell, V. Brabec, *Nucleic Acids Res.* **2005**, *33*, 5819–5828.
[15] Y. Jung, S. J. Lippard, *Chem. Rev.* **2007**, *107*, 1387–1407.
[16] S. R. Wedge, J. K. Porteous, E. S. Newlands, *Cancer Chemother. Pharmacol.* **1997**, *40*, 266–272.
[17] J. J. Warren, L. J. Forsberg, L. S. Beese, *Proc. Natl. Acad. Sci. USA* **2006**, *103*, 19701–19706.
[18] J. Klapacz, L. B. Meira, D. G. Luchetti, J. A. Calvo, R. T. Bronson, W. Edelmann, L. D. Samson, *Proc. Natl. Acad. Sci. USA* **2009**, *106*, 576–581.
[19] J. Jiricny, *Nat. Rev. Mol. Cell Biol.* **2006**, *7*, 335–346.

[20] Q. Fang, A. M. Noronha, S. P. Murphy, C. J. Wilds, J. L. Tubbs, J. A. Tainer, G. Chowdhury, F. P. Guengerich, A. E. Pegg, *Biochemistry* **2008**, *47*, 10892 – 10903.
[21] F. P. McManus, Q. Fang, J. D. Booth, A. M. Noronha, A. E. Pegg, C. J. Wilds, *Org. Biomol. Chem.* **2010**, *8*, 4414 – 4426.
[22] F. P. McManus, D. K. O'Flaherty, A. M. Noronha, C. J. Wilds, *Org. Biomol. Chem.* **2012**, *10*, 7078 – 7090.
[23] F. P. McManus, A. Khaira, A. M. Noronha, C. J. Wilds, *Bioconjugate Chem.* **2013**, *24*, 224 – 233.
[24] F. P. McManus, C. J. Wilds, *Toxicol. Res.* **2013**, *2*, 158 – 162.
[25] A. E. Pegg, *Chem. Res. Toxicol.* **2011**, *24*, 618 – 639.
[26] K. S. Srivenugopal, X. H. Yuan, H. S. Friedman, F. Ali-Osman, *Biochemistry* **1996**, *35*, 1328 – 1334.
[27] M. Xu-Welliver, A. E. Pegg, *Carcinogenesis* **2002**, *23*, 823 – 830.
[28] D. K. O'Flaherty, C. J. Wilds, *Chem. Eur. J.* **2015**, *21*, 10522 – 10529.
[29] R. T. Streeper, R. J. Cotter, M. E. Colvin, J. Hilton, O. M. Colvin, *Cancer Res.* **1995**, *55*, 1491 – 1498.
[30] S. J. Kim, C. Lester, T. P. Begley, *J. Org. Chem.* **1995**, *60*, 6256 – 6257.
[31] Y. J. Jian, L. Li, *J. Org. Chem.* **2013**, *78*, 3021 – 3029.
[32] S. Murata, Y. Mizumura, K. Hino, Y. Ueno, S. Ichikawa, A. Matsuda, *J. Am. Chem. Soc.* **2007**, *129*, 10300 – 10301.
[33] K. J. Bowman, R. L. Pla, Y. Guichard, P. B. Farmer, G. D. Jones, *Nucleic Acids Res.* **2001**, *29*, 101e.
[34] S. Park, M. Seetharaman, A. Ogdie, D. Ferguson, N. Tretyakova, *Nucleic Acids Res.* **2003**, *31*, 1984 – 1994.
[35] B. L. Gaffney, L. A. Marky, R. A. Jones, *Biochemistry* **1984**, *23*, 5686 – 5691.
[36] S. Kuzmich, L. A. Marky, R. A. Jones, *Nucleic Acids Res.* **1983**, *11*, 3393 – 3403.
[37] K. Abdu, M. K. Aiertza, O. J. Wilkinson, J. A. Grasby, P. Senthong, A. C. Povey, G. P. Margison, D. M. Williams, *Chem. Commun.* **2012**, *48*, 11214 – 11216.
[38] P. E. Verdemato, J. A. Brannigan, C. Damblon, F. Zuccotto, P. C. Moody, L. Y. Lian, *Nucleic Acids Res.* **2000**, *28*, 3710 – 3718.
[39] R. Coulter, M. Blandino, J. M. Tomlinson, G. T. Pauly, M. Krajewska, R. C. Moschel, L. A. Peterson, A. E. Pegg, T. E. Spratt, *Chem. Res. Toxicol.* **2007**, *20*, 1966 – 1971.
[40] D. S. Daniels, T. T. Woo, K. X. Luu, D. M. Noll, N. D. Clarke, A. E. Pegg, J. A. Tainer, *Nat. Struct. Mol. Biol.* **2004**, *11*, 714 – 720.
[41] J. Hu, A. Ma, A. R. Dinner, *Proc. Natl. Acad. Sci. USA* **2008**, *105*, 4615 – 4620.
[42] J. Butenandt, A. P. M. Eker, T. Carell, *Chem. Eur. J.* **1998**, *4*, 642 – 654.
[43] M. Tintoré, I. Gallego, B. Manning, R. Eritja, C. Fàbrega, *Angew. Chem. Int. Ed.* **2013**, *52*, 7747 – 7750; *Angew. Chem.* **2013**, *125*, 7901 – 7904.
[44] L. M. Hellman, T. J. Spear, C. J. Koontz, M. Melikishvili, M. G. Fried, *Nucleic Acids Res.* **2014**, *42*, 9781 – 9791.
[45] A. Keppler, S. Gendreizig, T. Gronemeyer, H. Pick, H. Vogel, K. Johnsson, *Nat. Biotechnol.* **2002**, *21*, 86 – 89.

Manuscript received: November 13, 2015
Accepted Article published: December 22, 2015
Final Article published: January 13, 2016